Chapter 2. Basic Atomic Physics

Academic and Research Staff

Professor Daniel Kleppner, Professor David E. Pritchard, Professor Wolfgang Ketterle, Professor Thomas J. Greytak, Dr. Hans-Joachim Miesner, Dr. Roberto Onofrio, Dr. Chandra S. Raman, Dr. Jörn Stenger, Dr. Lorenz Willmann

Visiting Scientists and Research Affiliates

Dr. Theodore W. Ducas,[1] Dr. Jana U. Lehner

Graduate Students

Michael R. Andrews, Ananth P. Chikkatur, Joel C. DeVries, Dallin S. Durfee, Dale G. Fried, Subhadeep Gupta, Jeffrey R. Holley, Shin Inouye, Thomas C. Killian, David A. Kokorowski, Christopher E. Kuklewicz, David Landhuis, Stephen C. Moss, Tony D. Roberts, Richard A. Rubenstein, Dan M. Stamper-Kurn

Undergraduate Students

Jeffrey C. Gore, Johnny M. Vogels,[2] Michael Köhl

Technical and Support Staff

Carol A. Costa

2.1 Bose-Einstein Condensation of Atomic Hydrogen

Sponsors

National Science Foundation
U.S. Navy - Office of Naval Research

Project Staff

Dale G. Fried, Thomas C. Killian, David Landhuis, Stephen C. Moss, Dr. Lorenz Willmann, Professor Thomas J. Greytak, Professor Daniel Kleppner

2.1.1 Introduction

During the past year, we finally succeeded in our search to observe Bose-Einstein condensation (BEC) in atomic hydrogen. The techniques for trapping and cooling hydrogen differ in many respects from those used to achieve BEC in alkali metal atoms, and we use a new tool for studying the condensate: high-resolution two-photon spectroscopy.

Bose-Einstein condensation is a pure quantum mechanical phase transition which takes place when the phase space density of a gas of atoms that obey Bose statistics is approximately unity. (Hydrogen and most alkali metal atoms obey Bose statistics because the electron and nucleus separately obey Fermi statistics.) The condition for condensation is[3]

$$n\Lambda_{th}^3 \geq 2.612 \quad (1)$$

Here n is the density and $\Lambda_{th} = \sqrt{2p\hbar^2 / k_B Tm}$ is the thermal De Broglie wavelength. When condensation occurs in an ideal system, a fraction of the gas drops into the system's ground quantum state: the atoms come to rest or, more precisely, to the zero point energy of the confining potential. In a real system, interactions between the atoms elevate the condensate's energy.

Bose-Einstein condensation was first observed with alkali metal atoms in 1995 by groups at JILA, MIT and Rice University.[4] The addition of hydrogen to the list of condensed atoms has attracted wide attention because of its different atomic properties and the dif-

1 Professor, Wellesley College, Wellesley, Massachusetts.

2 Eindhoven University of Technology, Eindhoven, The Netherlands.

3 K. Huang, *Statistical Mechanics*, 2nd ed. (New York: John Wiley, 1987).

4 M.H. Anderson, *Sci.* 269: 198 (1995); C.C. Bradley, *Phys. Rev. Lett.* 75: 1687 (1995); K.B. Davis, *Phys. Rev. Lett.* 75: 3969 (1995).

ferent conditions at the transition. In particular, the low mass of hydrogen permits a much higher transition temperature for a given atomic density n. Hydrogen also differs from other atoms in having an anomalously small s-wave scattering length, a. The weak repulsion between the atoms permits the creation of larger condensates than have been obtained in the alkali metal condensates. The elastic collision cross section $\sigma = 8\pi a^2$, is much smaller than in other atoms. The ultimate cooling step in hydrogen, as with all BEC atoms, is by evaporation, and the evaporation rate is limited by the elastic collision rate. Because of hydrogen's small cross section, evaporation proceeds relatively slowly.

The techniques for trapping and cooling hydrogen are described in detail elsewhere.[5] The source of cold atoms is a cryogenic RF-discharge operating at a temperature of 300 mK. The emerging atoms are confined in a cell of diameter 4 cm and length 60 cm. The binding energy of hydrogen to the surface is reduced to 1 K by covering the cell's walls with a film of superfluid ^{4}He. Superconducting coils in a "Ioffe-Pritchard" configuration provide a magnetic field with a minimum in the center of the cell. Atoms in the F = 1, m_F = 1 hyperfine state are trapped in the potential well while atoms in other hyperfine states are either expelled or suffer a large collisional loss rate. A maximum field of 0.9 T provides a magnetic trap depth of 0.5 K. The trapped atoms are in a metastable state, and collisions can induce spin-flips to lower-lying untrapped states. This dipolar decay is the main loss rate for trapped hydrogen. The two-body decay rate constant is 1.2×10^{-15} cm^3 s^{-1}.

Because the trapped atoms are not in thermal contact with the wall they can be cooled far below the cell temperature. Cooling is accomplished by evaporation. During collisions, some atoms receive enough energy to escape from the trap. If they happen to move through the region of a saddlepoint in the magnetic potential, they can leave. The average energy of the remaining atoms is reduced, and the system equilibrates to a lower temperature. The equilibrium temperature is a fraction of the trap depth, where the numerical value for hydrogen is typically 0.1. As the saddlepoint potential is lowered, the atoms cool. This must be done slowly enough for the gas to maintain thermal equilibrium. In addition, the time for an energetic atom to escape must be short compared to the time between collisions.

In our trap, the saddlepoint lies at the end of a long, thin volume, and the area for escape is small compared to the area of the trap. The time for an atom to escape depends on the trap's aspect ratio, and in our trap this can be as large as 400:1 for low temperatures. The potential experienced by the atoms becomes increasingly harmonic as the atoms cool and settle in the lowest region of the trap. This decouples the motion in different directions. As a result, an atom with a large excursion along the short axis of the trap can only slowly transform its motion into the axial direction, where it can escape. In such a case the atom is likely to collide before leaving the trap and fail to escape. In our trap, this effect limits the saddlepoint evaporation to temperatures of about 100 μK.

To overcome this problem, we employ an escape mechanism based on spin resonance,[6] first demonstrated for the alkali metal atoms.[7] A radio-frequency (RF) field is applied. Atoms that can reach the magnetic field in which they are in resonance are transferred to an untrapped state and leave the trap. This process does not depend on any particular direction of the motion of the atom, restoring the lost evaporation efficiency. Implementing RF evaporation in our low temperature apparatus required developing a non-metallic trapping cell compatible with the cryogenic environment.[8] Thermal conductivity of our all-plastic cell is provided by a 2 mm thick jacket filled with superfluid ^{4}He. The coils for generating the RF-field are wound directly on the plastic body. The fields are up to 2×10^{-7} T, and frequencies can range up to 46 MHz. Typically we switch to RF-ejection at a trap depth of 1.1 mK. This improvement allowed us to cool hydrogen into the quantum degenerate regime.

5 T.J. Greytak, *Bose-Einstein Condensation* (Cambridge, England: Cambridge University Press, 1995), p. 131.

6 D.E. Pritchard, K. Helmerson, and A.G. Martin, *Atomic Physics 11* (Singapore: World Scientific, 1989), p. 179.

7 W. Petrich, M.H. Anderson, J.R. Ensher, and E.A. Cornell, *Phys. Rev. Lett.* 74: 3352 (1995); K.B. Davis, M.O. Mewes, M.A. Joffe, M.R. Andrews, and W. Ketterle, *Phys. Rev. Lett.* 74: 5202 (1995).

8 D.G. Fried, *Bose-Einstein Condensation of Atomic Hydrogen*, Ph.D. diss., Department of Physics, MIT, 1999.

To study the trapped gas, we use high-resolution two-photon spectroscopy of the 1S-2S transition.[9] The transition is excited at 243 nm by a stabilized laser with a linewidth of about 1 kHz. The laser beam passes along the axis of the trap and is retro-reflected by a small mirror at the end of the trapping cell, providing a standing wave. The two-photon transition is essentially field-independent so that the transition is narrow even in an inhomogeneous magnetic field. Our detection scheme exploits the long lifetime of the metastable 2S-state, 122 ms. The transition is driven by a 0.4 ms-long laser pulse, and the excited atoms remain in the 2S state. They are quenched to the 2P state by applying an electric field pulse. The emitted Lyman-α photons are detected by a micro-channel plate.

Our advances in trapping and cooling allow us to study the system at increasing densities and decreasing temperatures. The narrow Doppler free transition, in which photons from the two counter-propagating beams are absorbed, allows us to measure the perturbation of the energy levels by the other atoms. Because the frequency shift is proportional to the density, this provides a powerful method for monitoring the density (Figure 1). The resulting frequency shift can be calculated from a collisional approach[10] or from a mean-field interaction picture.[11] The frequency shift is given by

$$\Delta\nu_{1S-2S} = (a_{1S\text{-}2S} - a_{1S-1S})\frac{4\hbar n_{1S}}{m} \qquad (2)$$

where $a_{g\text{-}e}$ is the s-wave scattering length for g state -e state atom interaction, the atom's mass is m, and n_{1S} is the density of ground state atoms. We have measured the frequency shift as a function of the density in our trap. The shape of the absorption spectrum (Figure 2) is dominated by the inhomogeneous density distribution due to the trapping potential. (The peak density in the trap can be determined independently by the density dependent loss due to dipolar decay from the trap.) We have observed the expected linear relation between density and frequency shift with a proportionality constant of χ = -3.8(8) x 10^{-10} Hz cm^3. With the theoretically well calculated value for $a_{1S\text{-}1S}$ = 0.0648 nm we can extract $a_{1s\text{-}2s}$ = -1.4(3) nm. This is in fair agreement with a recent calculation of -2.3 nm.[12] Once we have calibrated the cold collision frequency shift, we can use it to obtain the density distribution in our trap.

.

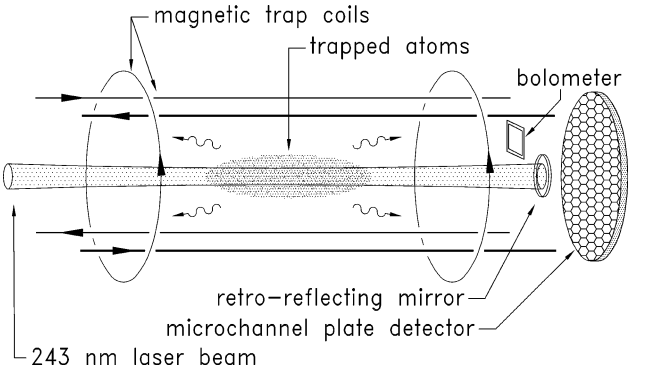

Figure 1. Schematic diagram of the apparatus. Coils create a magnetic field with a minimum along the trap axis, which confines the sample. The 243 nm laser beam is focused to a 50 μm beam radius and retroreflected. A 400 μs laser pulse promotes some atoms to the metastable 2S state. An electric field then Stark-quenches the 2S atoms, and the resulting Lyman-α fluorescence photons are counted by the microchannel plate. Not shown is the trapping cell which surrounds the sample and is thermally anchored to a dilution refrigerator. The actual trap is longer and narrower than indicated in the diagram.

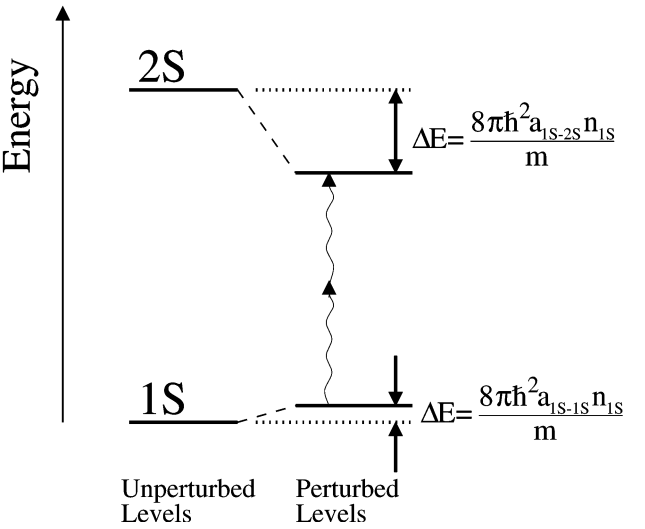

Figure 2. The energies of the atomic levels are perturbed by the presence of other atoms, proportional to the density n_{1S}. At low temperature, this can be described by the cold collision frequency shift with a single parameter, the s-wave scattering length a. We measure the shift in the transition energy by high-resolution two-photon spectroscopy.

9 C.L. Cesar, D.G. Fried, T.C. Killian, A.D. Polcyn, J.C. Sandberg, I.A. Yu, T.J. Greytak, D. Kleppner, and J.M. Doyle, *Phys. Rev. Lett.* 77: 255 (1996).

10 B.J. Verhaar, J.M.V.A. Koelman, H.T.C. Stoof, and O.J. Luiten, *Phys. Rev. A* 35: 3825 (1987).

11 R.K. Pathria, *Statistical Mechanics* (New York: Pergamon Press, 1972), p. 300.

12 M.J. Jamieson, A. Dalgarno, and J.M. Doyle, *Mol. Phys.* 87: 817 (1996).

In addition to Doppler-free excitation, the 1S-2S transition can be excited by two co-propagating photons, yielding a Doppler-broadened line. In addition to the Doppler broadening, the transition is shifted because of the photon-recoil energy that must be provided to the atoms as a whole. The recoil velocity is about 3 m/s and induces a blue shift of the transition of 6.7 MHz. Our experiments have displayed the Doppler profile for hydrogen's 1S-2S transition for the first time. Assuming a Maxwell-Boltzmann velocity distribution, the rms width of the spectrum provides a direct measure of the temperature of the sample. The width is about 2 MHz for a temperature of 40 μK.

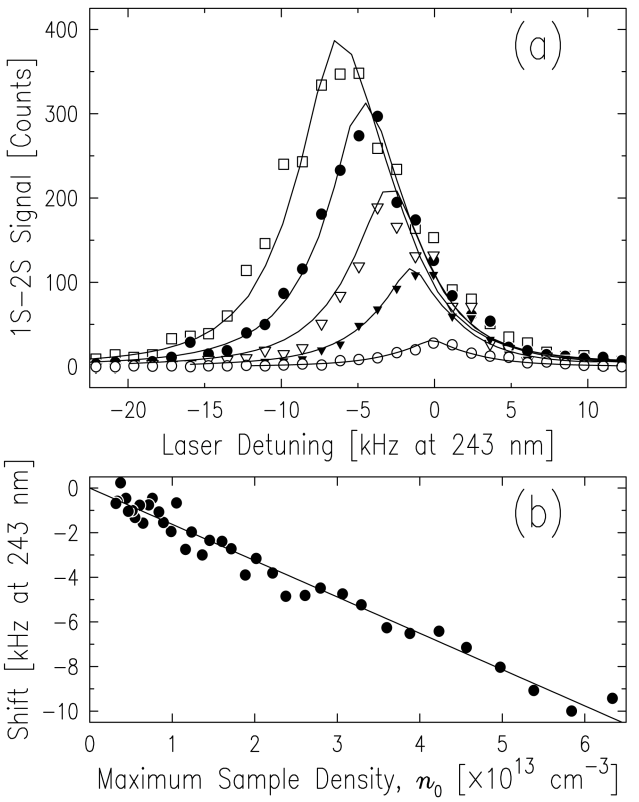

Figure 3. (a) The spectrum of the 1S-2S transition frequency at different densities. For a high density, the signal is larger because there are more atoms in the trap and is further red-shifted by the cold collision frequency shift. The solid lines are model calculations taking the density distribution into account. (b) The center of the line shows a linear dependence on the density.

Bose-Einstein condensation results in a macroscopic population of the lowest momentum state of the trap. Condensation results in a large narrow spectral feature at the center of the Doppler profile (Figure 3). Due to the cold collision frequency shift, the condensate's spectrum is red-shifted and broadened. This shift also allows us to observe the condensate in the Doppler-free excitation, causing it to be red-shifted further than the normal gas signal. The spectra from Doppler-free and Doppler-sensitive excitation have the same width, indicating that we are, in fact, observing condensation in momentum space.

The primary loss mechanism, dipolar decay, limits the condensate fraction to a few percent. We determine the density in the condensate from the maximum frequency shift, 0.6 MHz, which corresponds to a density of 3×10^{15} cm^{-3}. The number of condensed atoms is found from the density and the known geometry of the trap. For the data shown in Figure 4 the number is 10^9 atoms. The density of the normal gas at the transition, found from its frequency shift, is 2×10^{14} cm^{-3}. The temperature at the transition is found from the width of the Doppler profile and is 60(20)μK.

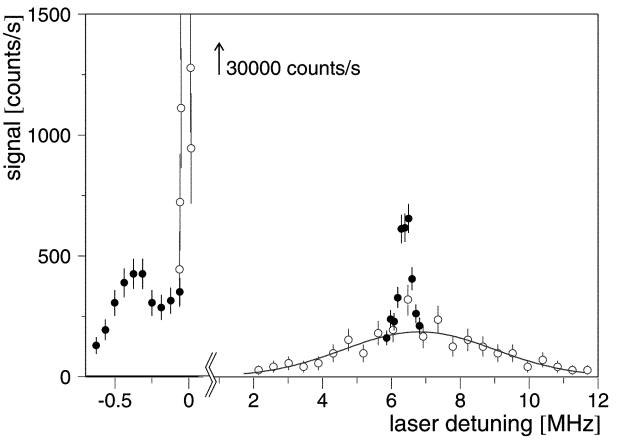

Figure 4. Spectrum of magnetically trapped atomic hydrogen in the presence of a condensate. The spectra at positive detainees are from absorption of two co-propagating photons. It reflects the momentum distribution in the trap. Bose-Einstein condensation is a macroscopic population of the lowest momentum state. Thus its signal is near the center of the broad Doppler profile. It is shifted and broadened by the cold collision frequency shift. In addition, this shift allows us to observe the condensate by Doppler-free absorption of two counter propagating photons. Its signature is the large red-shift indicating a region of high density. (Note, that the frequency scale changes near the origin.)

Now that the goal of observing BEC has been achieved, the way is open to major improvements in the technique. We believe that it is possible to make much larger condensates and to observe them with much higher detection efficiency. In addition to making it possible to study BEC in a new medium, our advances raise the possibility of making an intense coherent atom source and open the way to numer-

ous atomic studies including atomic collision processes in hydrogen's metastable state and interactions in more highly excited states. Furthermore, our development of 1S-2S Doppler-free spectroscopy of cold trapped hydrogen opens the way to a major improvement in the precision of one of the most interesting energy intervals in atomic physics.

2.1.2 Journal Articles

Fried, D.G., T.C. Killian, L. Willmann, D. Landhuis, S.C. Moss, T.J. Greytak, and D. Kleppner. "Bose-Einstein Condensation of Atomic Hydrogen." *Phys. Rev. Lett.* 81(18): 3811 (1998).

Killian, T.C., D.G. Fried, L. Willmann, D. Landhuis, S.C. Moss, T.J. Greytak, and D. Kleppner. "Cold Collision Frequency Shift of the 1S-2S Transition in Hydrogen." *Phys. Rev. Lett.* 81(18): 3807-10 (1998).

2.1.3 Doctoral Dissertations

Killian, T.C. *Cold Collision Frequency Shift of the 1S-2S Transition in Atomic Hydrogen*. Ph.D. diss. Department of Physics, MIT, 1999.

Fried, D.G. *Bose-Einstein Condensation of Atomic Hydrogen.* Ph.D. diss. Department of Physics, MIT, 1999.

2.2 Determination of the Rydberg Frequency

Sponsor

National Science Foundation
Grant PHY 96-024740

Project Staff

Joel C. DeVries, Dr. Theodore W. Ducas, Jeffrey R. Holley, Professor Daniel Kleppner

The Rydberg frequency, cR_∞ sets the frequency scale for the spectrum of hydrogen atoms. From a frequency measurement of one transition in hydrogen, cR_∞ can be extracted, and the frequency of any other transition can be predicted, assuming the relativistic, QED, and proton structure corrections can be computed to the desired accuracy. Recent advances in optical frequency techniques have made possible measurements of cR_∞ at better than 1 part in 10^{11}.[13]

The goal of this experiment is to measure the frequency of a particular transition in atomic hydrogen which is not in the optical but the millimeter-wave region of the hydrogen spectrum. This transition is between two highly excited "circular Rydberg" states, each with a principal quantum number, n, between 27 and 30. The QED and proton structure corrections to these states are small and are not a barrier to extracting the Rydberg frequency to our accuracy goal of 1 part in 10^{11}. The frequencies of transitions between these circular Rydberg states are relatively small, around 300 GHz, and can easily be measured with respect to a cesium clock. The optical measurements, in contrast, rely on intermediate standards which have been previously calibrated and on separate measurements to account for QED and proton structure corrections. Thus our result will be an independent check, in a different regime, of the optical measurements. Furthermore, our measurement will help provide a frequency calibration of the spectrum of hydrogen, enabling the creation of a comprehensive frequency standard extending from the radio frequency regime to the ultraviolet.

The experiment employs an atomic beam configuration to reduce Doppler and collisional perturbations. Atomic hydrogen is excited to the low angular momentum n = 27 or 29, m = 0 state by two-photon stepwise absorption. The excited atoms are then transferred to the longer lived n = 27, |m| = 26 or n=29, |m| = 28 "circular" state by absorption of circularly polarized radio frequency radiation.[14] The atoms enter a region of uniform electric field in which the frequency of the transition (n = 27, |m| = 26) $\rightarrow$(n=28, |m| = 27) or (n = 29, |m| = 28) $\rightarrow$(n = 30, |m| =29) is measured by the method of separated oscillatory fields. The final state distribution is analyzed by a state-sensitive electric field ionization (EFI) detector. The resonance signal appears as a transfer of atoms from the lower state to the upper state as the millimeter-wave frequency is tuned across the transition.

13 B. de Behavior, "Absolute Frequency Measurement of the 2S-8S/D Transitions in Hydrogen and Deuterium: New Determination of the Rydberg Constant," *Phys. Rev. Lett.* 78(3): 440-43 (1997); T. Udem, "Phase-Coherent Measurement of the Hydrogen 1S-2S Transition Frequency with an Optical Frequency Interval Divider Chain," *Phys. Rev. Lett.* 79(14): 2646-49 (1997).

14 R. Lutwak, J. Holley, P.P. Chang, S. Paine, D. Kleppner, and T. Ducas, "Circular States of Atomic Hydrogen," *Phys. Rev. A* 56(2): 1443-52 (1997).

Figure 5 and Figure 6 illustrate the main features of the apparatus. Atomic hydrogen or deuterium is dissociated from H_2 or D_2 in a radio frequency discharge. The beam is cooled by collisions with a cryogenic thermalizing channel in order to slow the atoms and thereby increase the interaction time. After the beam is collimated, the atoms pass through two layers of magnetic shielding and an 80 K cryogenic shield before entering the interaction region. The interaction region is logically divided into three sections: the circular state production, separated fields, and detection regions. These are described briefly in the following.

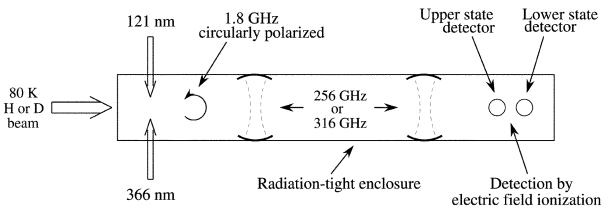

Figure 5. Schematic top view of the apparatus.

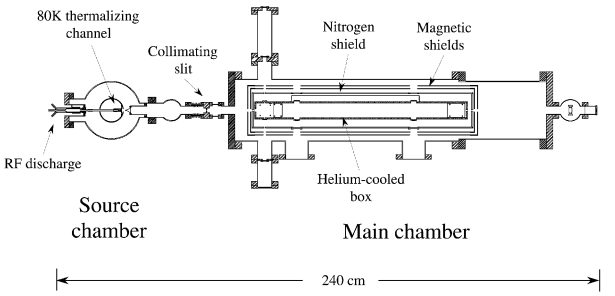

Figure 6. Top view of the atomic beam vacuum apparatus.

In the circular state production region, the hydrogen atoms are excited from the 1s ground state, through the $2p_{3/2}$ state, to the n = 27 or 29, m = 0 state by two-photon stepwise excitation. The laser system has been detailed in the 1995 and 1996 *RLE Progress Reports*. The optical excitation is performed in an electric field to provide selective population of a particular m = 0 level. The electric field is then rapidly reduced to an intermediate value as the atoms pass through the center of a circle of four electrodes. The antennas are fed by a 1.8 GHz RF source with a 90° phase delay between adjacent pairs. This creates a circularly polarized field which drives the atoms into the n = 27, |m| = 26 or n = 29, |m| = 28 circular state through a multiphoton absorption process. A pulsed EFI detector in the circular state production region monitors the efficiency of the optical excitation and angular momentum transfer processes.

After the atoms are prepared in the circular Rydberg state, the beam enters the millimeter-wave separated fields region. Because Rydberg atoms interact strongly with external fields, accurate measurement of the energy level structure requires careful control of the interaction environment. Thermal radiation is reduced by cooling the entire interaction region to ≈ 4 K with a liquid helium flow system. The ambient magnetic field is reduced by the double-wall high-permeablility shields. A small electric field, which defines the quantization axis of the atoms, is applied with high uniformity by field plates above and below the atomic beam. The millimeter-waves intersect the atomic beam at two locations separated by 50 cm. The millimeter-wave optical system was described in the 1990 *RLE Progress Report*. The millimeter-wave zones inside the interaction region consist of two Fabry-Perot cavities which will be described below.

The state distribution of the atoms emerging from the interaction region is analyzed by a state-selective EFI detector. Within the detector, the atoms enter a region of increasing electric field produced by a pair of symmetric ramped plates held at constant potential. Atoms in different states are selectively ionized at different fields, and the charged nuclei are detected at different positions. The detection electronics record the state and arrival time of each atom to reach the detector. Because the laser system is pulsed, the time resolution of the ionization signal allows contributions to the resonance pattern from each velocity class to be analyzed individually, providing a valuable check on possible systematic errors.

To find the frequency of the circular state to circular state transition, we measure the population inversion as the millimeter-waves are tuned through resonance. The inversion is defined as

$$I = \frac{N_{upper} - N_{lower}}{N_{upper} + N_{lower}} \tag{3}$$

where N_{lower} and N_{upper} are the number of ion counts detected in each electron multiplier. As a preliminary diagnostic step, we can leave open only one of the millimeter-wave ports, in which case the resonance curve is a single peak—a “Rabi curve.” If both milli-

meter-wave ports are open, we see the interference fringe characteristic of the Ramsey separated oscillatory fields technique.

This year we have concentrated on the elimination of systematic errors in our measurement of the Rydberg frequency. We have increased the signal rate to the point that our statistical error is about 3 parts in 10^{11} for one day of data acquisition. This allows us to vary parameters and make a reasonably accurate determination of their effect on the data. Parameters we have varied include the static electric field, magnetic field, intensity of the atomic beam, polarization of the excitation lasers, RF power used in the circularization process, method of applying the millimeter-wave radiation to the atoms, and time standard employed for the frequency measurement. This work has allowed us to identify and control some of the sources of systematic error.

The most conspicuous systematic error was evident as broad wings on the Rabi resonance curves due to millimeter-wave radiation which (1) scattered off the box's entrance and exit apertures or (2) was not properly absorbed in the beam dumps. To resolve this problem, we installed two confocal Fabry-Perot cavities to confine the radiation and give it a well-characterized spatial mode. The cavities employ a novel design for the input coupler. Normally a small hole in the center of a mirror is used to couple the radiation into the cavity. This approach was not acceptable because too much of the incoming radiation would be scattered out of the cavity. Instead, we used an epoxy to adhere a 500 line/inch copper mesh to the concave surface of a lens. This produced a highly reflective, spherical surface that efficiently couples radiation into the cavity. The introduction of these cavities greatly reduced the scattered millimeter-wave radiation inside the box enclosure. This in turn produced a vast improvement in the symmetry of the Rabi curves as can be seen in Figure 7 which compares results with the running wave geometry and the cavity geometry.

The second major systematic problem was an asymmetry of the Ramsey fringes due to polarization of the electron spins in the hydrogen beam. This polarization produces an uncertainty in our measurement because it affects the relative weighting of two fine structure transitions, which we do not completely resolve. We have found that a small magnetic field (50 milligauss) applied in the production region reduces the polarization to less than one or two percent, thereby reducing the associated uncertainty in the extracted Rydberg frequency to an acceptable level. Figure 8 shows a typical Ramsey fringe taken under these conditions.

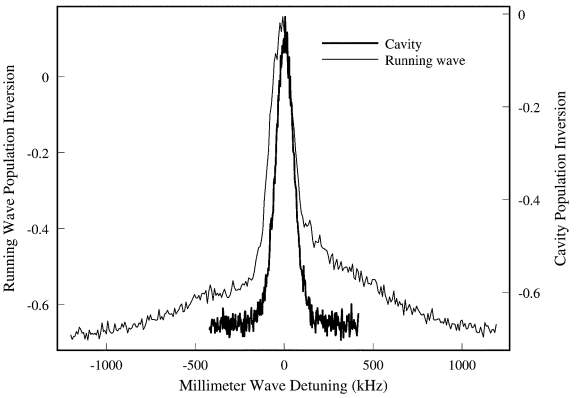

Figure 7. Comparison of Rabi curves for running wave and cavity geometries.

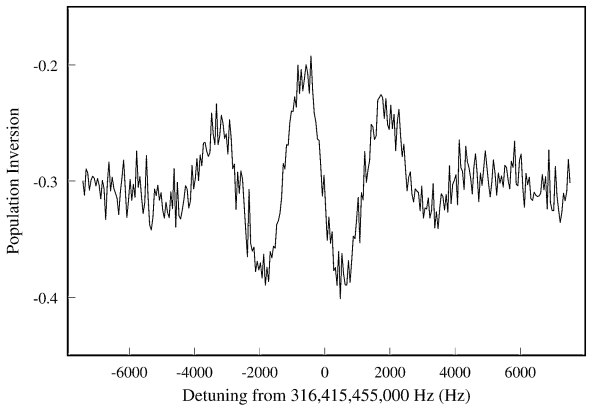

Figure 8. Ramsey fringe for the n = 27 $\rightarrow$n = 28 transition in hydrogen, with a 50 milligauss magnetic field applied in the production region. The fitted electron spin polarization is less than about one or two percent.

We are now concerned with understanding the electric fields in the interaction region. It is necessary to apply a uniform electric field, large compared to any stray fields, in order to orient the circular state atoms. The electric field causes a quadratic shift in the transition frequency. By varying the strength and direction of the applied electric field, we may extrapolate to the zero-field frequency (see Figure 9). However, it is still possible for stray fields to skew the result. Thus we have taken care to reduce charge buildup on the exposed surfaces in the interaction region. We can use information from electric field-sensitive tran-

sitions between near-circular states, as well as from the scaling of the quadratic Stark shift with n, to check that the uncertainty from stray fields is small.

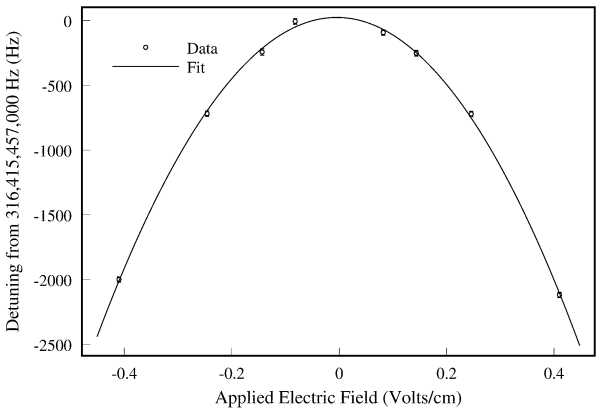

Figure 9. Variation with applied electric field of the center frequencies of eight separate Ramsey fringes.

With these measures in place to reduce systematic errors, we are now continuing to acquire resonance data and check the reproducibility of our Rydberg frequency measurements. The accumulation of several experimental runs will allow us to approach an uncertainty of 1 part in 10^{11}.

2.2.1 Doctoral Dissertation

Holley, J.R. *Precision Spectroscopy of Circular Rydberg States of Hydrogen*. Ph.D. diss. Department of Physics, MIT, 1998.

2.3 Atom Interferometry

Sponsors

Joint Services Electronics Program
Grant DAAG55-98-1-0080
National Science Foundation
Grant PHY 95-14795
U.S. Army Research Office
Grant DAAH04-94-G-0170
Grant DAAG55-97-1-0236
Grant DAAH04-95-1-0533
Grant DAAG55-98-1-0429
U.S. Navy - Office of Naval Research
Contract N00014-96-1-0432

Project Staff

Richard A. Rubenstein, David A. Kokorowski, Tony D. Roberts, Subhadeep Gupta, Dr. Jana U. Lehner, Professor David E. Pritchard

2.3.1 Introduction

Atom interferometers, in which atom or molecule de Broglie waves are coherently split and then recombined to produce interference fringes, have opened up exciting new possibilities for precision and fundamental measurements of complex particles. The ability to accurately measure interactions that displace the de Broglie wave phase has led to qualitatively new measurements in atomic and molecular physics, fundamental tests of quantum mechanics, and new ways to measure acceleration and rotation:

- Atom interferometers permit completely new investigations of atoms and molecules including precision measurement of atomic polarizabilities that test atomic structure models, determination of long range forces important in cold collisions and Bose-Einstein condensation, and measurement of molecular polarizability tensor components.
- Atom interferometers can make fundamental investigations in quantum mechanics. These include measurement of topological and geometric phases, quantum decoherence, and investigations of multiparticle interferometry and entanglement.
- The large mass and low velocities of atoms makes atom interferometers especially useful in inertial sensing applications, both as precision accelerometers and as gyroscopes. They have a potential sensitivity to rotations ~10^{10} greater than in optical interferometers of the same area.
- Atom interferometers may have significant applications to measurement of atom-surface interactions in condensed matter physics.
- Atom interferometers may have uses in lithography using coherently manipulated fringe patterns that are directly deposited onto substrates.
- Atomic clocks are essentially sensitive longitudinal atom interferometers, capable of easily measuring phase shifts due to velocity changes of 1 part in 10^{10}.

Our group has pioneered many of these areas, including the first atom interferometry experiments that employed physically separated paths to make

precision measurements,[15] the first quantitative demonstration of an atom interferometer inertial sensor,[16] and a unique longitudinal atom interferometer.[17]

2.3.2 Longitudinal Atom Interferometry

Over the past year, we have performed a series of atom optical experiments using a new longitudinal interferometer (see Figure 10). In this interferometer, which consists of a pair of differentially detuned, separated oscillatory fields (DSOF), the two interfering paths are separated in longitudinal momentum space rather than position space (the usual case in matter-wave interferometry). In the first experiment,[17] we demonstrated that the velocity-induced dephasing of an amplitude modulated atomic beam can be reversed, using DSOF, in a process analogous to half a spin echo. Turning the process around, we were able to produce "remote" amplitude modulation at any desired location in the beam. We went on to measure the quantum state of a beam which had been non-trivially modulated[18] in the first demonstration of our general technique for using DSOF to determine the longitudinal density matrix of such systems.[19] Finally, we performed a search of our supersonic beam source,[20] looking for evidence of inherent coherences which would be undetectable using conventional techniques. The results of this last experiment have resolved a long standing controversy over the correct quantum description of the atomic beams used in all sorts of atomic physics experiments. We have also developed a fully quantum mechanical formalism[19] for describing molecular beam resonance. This formalism provides a perspective on the resonance phenomena which should lead to further theoretical and experimental advances in the area of longitudinal atom optics.

Rephased Amplitude Modulation

When high-frequency (> 100 kHz) amplitude modulation is applied to our atomic beam, the "packets" of atoms produced quickly begin to overlap due to the distribution of their atomic velocities. A detector placed more than a few centimeters downstream will see no evidence of the modulation, but instead simply a constant flux of atoms. The DSOF interferometer, however, introduces a velocity dependent phase shift that can be tailored to cancel this natural dephasing. This allows us to detect the "hidden" amplitude modulation, which appears as a time-independent interference signal easily observed by a slow detector with no response above 5 kHz.

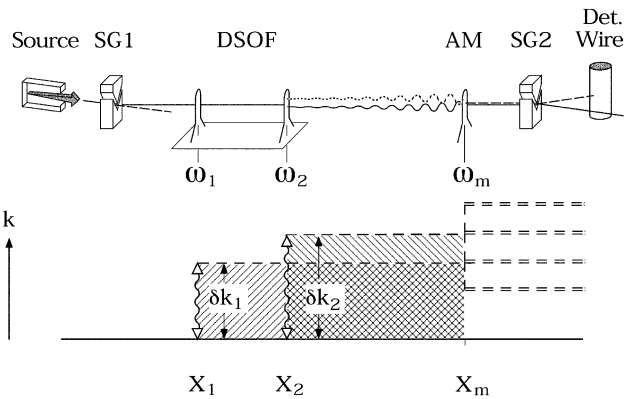

Figure 10. Longitudinal interferometer: the interfering paths are separated in momentum and internal state space, rather than position space. Atoms incident in the ground state are excited either in the first or second of two differentially detuned separated oscillatory fields (DSOF) coils. As the atoms are excited, they also receive a momentum kick proportional to the detuning of the field coil from resonance. Beyond the second region, the two paths overlap to produce an interference pattern.

Measuring the Density Matrix of a Matter-Wave Beam

As indicated above, amplitude modulation of an atomic beam can be detected using the DSOF interferometer. The exact nature of the resulting interfer-

15 D.W. Keith, C.R. Ekstrom, Q.A. Turchette, and D.E. Pritchard, "An Interferometer for Atoms," *Phys. Rev. Lett.* 66(21): 2693-96 (1991).

16 A. Lenef, T.D. Hammond, E.T. Smith, M.S. Chapman, R.A. Rubenstein, and D.E. Pritchard, "Rotation Sensing with an Atom Interferometer," *Phys. Rev. Lett.* 78(5): 760-63 (1997).

17 E.T. Smith, A. Dhirani, D.A. Kokorowski, R.A. Rubenstein, T.D. Roberts, H. Yao, and D.E. Pritchard, "Velocity Rephased Longitudinal Momentum Coherences with Differentially Detuned Separated Oscillatory Fields," *Phys. Rev. Lett.* 81(10): 1996-99 (1998).

18 R.A. Rubenstein, D.A. Kokorowski, A. Dhirani, T.D. Roberts, S. Gupta, J. Lehner, W.W. Smith, E.T. Smith, H.J. Bernstein, and D.E. Pritchard, "Measurement of the Density Matrix of a Longitudinally Modulated Atomic Beam," submitted to *Phys. Rev. Lett.*

19 D.E. Pritchard, R.A. Rubenstein, A. Dhirani, D.A. Kokorowski, E.T. Smith, T.D. Hammond, and B. Rohwedder, "Longitudinal Atom Optics Using Localized Oscillating Fields: A Fully Quantum Mechanical Treatment," *Phys. Rev. A*, forthcoming.

20 R.A. Rubenstein, A. Dhirani, D.A. Kokorowski, T.D. Roberts, E.T. Smith, W.W. Smith, H.J. Bernstein, J. Lehner, S. Gupta, and D.E. Pritchard, "Search for Off-diagonal Density Matrix Elements for Atoms in a Supersonic Beam," *Phys. Rev. Lett.*, forthcoming.

ence pattern encodes a great deal of information about the amplitude modulator itself. The modulation frequency can be deduced by the relative detunings of the two DSOF coils, and the modulator's location can be inferred from the average detuning. We have actually gone much further in characterizing the modulation, however. A Fourier transform of the interference fringes determines a slice of the atomic density matrix. Building up the entire density matrix we obtained a complete set of knowable information about the quantum state of our atomic beam. In a recently completed experiment, we measured the density matrix of a beam that had been doubly amplitude modulated. In Figure 11 our results are plotted showing "slices" of the density matrix for this system, as determined using our DSOF interferometer.

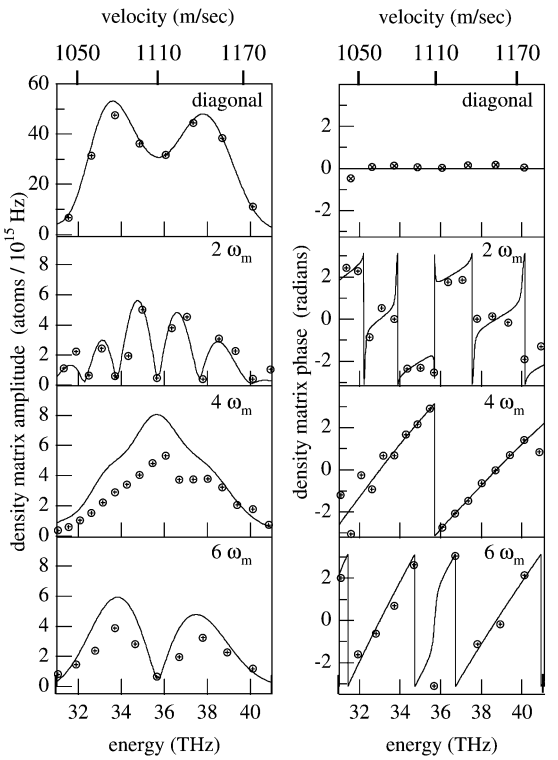

Figure 11. Measured amplitude (a) and phase (b) of the doubly amplitude modulated density matrix with modulation frequency $\omega_m = 2\pi \times 60.9$ kHz. The solid lines are a theoretical predictions based on the parameters of the modulation.

Searching for Coherences

Using the same Fourier transform technique as in the density matrix measurement, we have performed a search of our atomic beam source for any intrinsic momentum coherences (which would appear as amplitude modulation) up to a frequency of 100 kHz. To do this, we simply looked for interference fringes at all possible modulation frequencies. Our data primarily indicate the absence of any such intrinsic modulation. This confirms a long standing, yet never proven, assumption that the density matrix of an atomic beam is essentially diagonal—that is, there are no detectable correlations between different momentum components of the beam. This implies that there is no regular emission of wavepackets from the oven, for example. This knowledge will be important to the field of atom optics as we attempt to exert ever finer control over the quantum state of atomic beams (e.g., in atom lithography).

2.3.3 Ongoing Investigations

While pursuing the longitudinal interferometry experiments described above, we have also made significant upgrades to our transverse interferometer apparatus, including increased vibrational and thermal isolation and a redesigned vacuum chamber which provides greater access to the experimental components. Having made these improvements, we plan now to emphasize new and more precise measurements in atomic physics as well as fundamental experiments in quantum mechanics. Exploiting the capability of our separated beam interferometer to apply well-defined interactions to only one arm of the interferometer, we aim to significantly improve our knowledge of atomic and molecular properties that are inaccessible by any other experimental means.

Polarizability of Multiple Alkalis

The polarizability of an atom governs its interaction with electric fields and is an important parameter in Van der Waals interactions, electric dipole transition rates, and long-range interatomic potentials. We will measure the polarizabilities of the alkali metals through cesium to <0.1% accuracy—more than an order of magnitude better than current values—to measure their relative polarizability at the 0.01% level. The species-independence of our gratings versus light gratings allows us to switch alkalis easily, and velocity multiplexing will increase our accuracy and precision to the 0.1% and 0.01% targets. Our relative measurements will ultimately be normalized by a single, higher precision experiment using a sodium BEC.

Anisotropic Polarizability of Sodium Molecules

We will also make the first measurement of both parallel and perpendicular components of the polarizability of the dimer molecule Na_2. This will permit

tests of various approximations used in molecular structure calculations. The asymmetry of the polarizability causes the electric field-induced phase shift to depend on the molecule's rotational state. The beating of interference patterns for molecules in different rotational states generates considerable structure as a function of field strength and permits accurate determination of both polarizability components.

Velocity Dependent Index of Refraction

We were the first to investigate the index of refraction of gasses for sodium matter waves by measuring the phase shift when the sodium (and molecular sodium) de Broglie waves in one arm of our interferometer passed through a gas cell.[21] We now propose to extend our study by varying the velocity of our sodium beam to adjust the average center of mass energy of the inter-atomic collisions and to reduce the uncertainty in center-of-mass energy by cooling the gas cell to liquid nitrogen temperatures. In optical terminology, we will measure the dispersion, i.e., the variation of index with wavelength. These measurements will refine the shapes of the long-range potentials between sodium and other gases and test the new theoretical predictions inspired by our earlier work. We hope to observe glory oscillation, a novel interference effect which manifests as oscillations in the index of refraction as a function of velocity.[22]

Decoherence

In a recent experimental realization[23] of Feynman's *gedanken* experiment, we explicitly demonstrated that the loss of interference due to scattering a single photon from an atom in our interferometer is directly related to the degree of "which-path" information contained in the final state of the scattered photon. While this supports the general picture of decoherence as "monitoring by the environment," theorists warn[24] that the intuition derived from simple experiments does not necessarily extend to cover more realistic systems such as might be encountered in quantum computers. We will extend our previous experiment to approach the limit of a single quantum object interacting with a thermal environment (i.e., blackbody radiation), the mechanism most often invoked to explain the fragility of superposition states in quantum computation.

2.3.4 Publications

Kokorowski, D.A., A. Dhirani, T.D. Hammond, B. Rohwedder, R.A. Rubenstein, E.T. Smith, and D.E. Pritchard. "Fully Quantized Treatment of Molecular Beam Resonance." *Fortschr. Phys.* 46(6-8): 849-53 (1998).

Pritchard, D.E., M.S. Chapman, T.D. Hammond, D.A. Kokorowski, A. Lenef, R.A. Rubenstein, E.T. Smith, and J. Schmiedmayer. "Atom Interferometers and Atomic Coherence." *Fortschr. Phys.* 46(6-8): 801-08 (1998).

Pritchard, D.E., R.A. Rubenstein, A. Dhirani, D.A. Kokorowski, E.T. Smith, T.D. Hammond, and B. Rohwedder. "Longitudinal Atom Optics Using Localized Oscillating Fields: A Fully Quantum Mechanical Treatment." *Phys. Rev. A.* Forthcoming.

Rubenstein, R.A., A. Dhirani, D.A. Kokorowski, T.D. Roberts, E.T. Smith, W.W. Smith, H.J. Bernstein, J. Lehner, S. Gupta, and D.E. Pritchard. "Search for Off-diagonal Density Matrix Elements for Atoms in a Supersonic Beam." *Phys. Rev. Lett.* Forthcoming.

Smith, E.T., A. Dhirani, D.A. Kokorowski, R.A. Rubenstein, T.D. Roberts, H. Yao, and D.E. Pritchard. "Velocity Rephased Longitudinal Momentum Coherences with Differentially Detuned Separated Oscillatory Fields." *Phys. Rev. Lett.* 81(10): 1996-99 (1998).

2.3.5 Doctoral Dissertation

Rubenstein, R.A. *Longitudinal Atom Optics: Measuring the Density Matrix of a Matter Wave Beam.* Ph.D. diss. Department of Physics, MIT, 1998.

21 J. Schmiedmayer, M.S. Chapman, C.R. Ekstrom, T.D. Hammond, S. Wehinger, and D.E. Pritchard, "Index of Refraction of Various Gases for Sodium Matter-waves," *Phys. Rev. Lett.* 74: 1043 (1995).

22 E. Audouard, P. Duplaa, and J. Vigue, "Glory and Resonance Effects in the Index of Refraction for Atomic Waves," *Europhys. Lett.* 32: 397-400 (1995).

23 M.S. Chapman, T.D. Hammond, A. Lenef, J. Schmiedmayer, R.A. Rubenstein, E. Smith, and D.E. Pritchard, "Photon Scattering from Atoms in an Atom Interferometer: Coherence Lost and Regained," *Phys. Rev. Lett.* 75: 3783 (1995).

24 J.R. Anglin, J.P. Paz, and W.H. Zurek, "Deconstructing Decoherence," *Phys. Rev. A* 55: 4041-53 (1997).

2.4 Cooling and Trapping Neutral Atoms

Sponsors

National Aeronautics and Space Administration
Grant NAG8-1435
National Science Foundation
Grant PHY 95-01984

David and Lucile Packard Foundation
Grant 96-5158
U.S. Army Research Office
Agreement DAAG55-98-1-0080
U.S. Navy - Office of Naval Research
Contract N00014-96-1-0485
AASERT Grant N00014-94-1-0807
AASERT Grant N00014-95-1-1121

Project Staff

Professor Wolfgang Ketterle, Dr. Hans-Joachim Miesner, Dr. Roberto Onofrio, Dr. Chandra S. Raman, Dr. Jörn Stenger, Michael R. Andrews, Ananth P. Chikkatur, Dallin S. Durfee, Shin Inouye, Christopher E. Kuklewicz, Dan M. Stamper-Kurn, Jeffrey C. Gore, Johnny M. Vogels, Michael Köhl, Carol A. Costa

2.4.1 Introduction

The observation of Bose-Einstein condensation (BEC) in dilute atomic gases[25] was the realization of many long-standing goals: (1) to cool neutral atoms into the ground state of the system, thus exerting ultimate control over the motion and position of atoms limited only by Heisenberg's uncertainty relation; (2) to generate a coherent sample of atoms all occupying the same quantum state (this was subsequently used to realize an atom laser, a device which generates coherent matter waves); and (3) to create a quantum fluid with properties quite different from the quantum liquids He-3 and He-4. This provides a testground for many-body theories of the dilute Bose gas which were developed many decades ago but never tested experimentally. Bose-Einstein condensates offer intriguing possibilities for further research. They are predicted to show superfluidity and other manifestations of coherent behavior and are likely to find use in a variety of applications, e.g., atom interferometry, precision measurements, and atom optics.

Our focus in 1998 was experiments with optically trapped Bose-Einstein condensates. In the previous year, we had realized pure optical confinement of a condensate,[26] thus eliminating the limitations of magnetic trapping for further studies of BEC. Magnetic traps require large-scale inhomogeneous magnetic fields which might interfere with applications in precision atom optics. For example, in the first demonstration of an atom laser,[27] coherent atomic pulses were coupled out into an inhomogeneous magnetic field which served to confine the remaining condensate. Thus, during propagation, the pulses were exposed to Zeeman shifts. While these shifts were mitigated by producing $m_F = 0$ atoms, quadratic Zeeman shifts may preclude precision experiments on such pulses.

The unprecedented control over the motion and position of neutral atoms realized by BEC should offer major advantages for metrology. However, magnetic traps cannot trap atoms in the "non-magnetic" $m_F = 0$ state, which is preferable for atomic clocks and other precision experiments, thus limiting the use of trapped condensates for metrology.

More generally, magnetic traps can confine only weak-field seeking hyperfine states. Since the atomic ground state is always strong-field seeking, weak-field seeking states can inelastically scatter into the ground state (dipolar relaxation) resulting in heating and trap loss. This restriction to weak-field seeking states also limits the use of BEC for studies of various atomic properties which depend crucially on the hyperfine state, such as collision resonances, or for examinations of condensates composed of various combinations of hyperfine states.

---

25 M.H. Anderson, J.R. Ensher, M.R. Matthews, C.E. Wieman, and E.A. Cornell, "Observation of Bose-Einstein Condensation in a Dilute Atomic Vapor," *Sci.* 269: 198 (1995); K.B. Davis, M.-O. Mewes, M.R. Andrews, N.J. van Druten, D.S. Durfee, D.M. Kurn, and W. Ketterle, "Bose-Einstein Condensation in a Gas of Sodium Atoms," *Phys. Rev. Lett*. 75: 3969 (1995); C.C. Bradley, C.A. Sackett, and R.G. Hulet, "Bose-Einstein Condensation of Lithium: Observation of Limited Condensate Number," *Phys. Rev. Lett.* 78: 985 (1997).

26 D.M. Stamper-Kurn, M.R. Andrews, A.P. Chikkatur, S. Inouye, H.-J. Miesner, J. Stenger, and W. Ketterle, "Optical Confinement of a Bose-Einstein Condensate," *Phys. Rev. Lett*. 80: 2072 (1998).

27 M.R. Andrews, C.G. Townsend, H.-J. Miesner, D.S. Durfee, D.M. Kurn, and W. Ketterle, "Observation of Interference Between Two Bose Condensates," *Sci.* 275: 637 (1997); M.-O. Mewes, M.R. Andrews, D.M. Kurn, D.S. Durfee, C.G. Townsend, and W. Ketterle, "Output Coupler for Bose-Einstein Condensed Atoms," *Phys. Rev. Lett*. 78: 582 (1997).

These limitations have led us to the development of an all-optical trap for Bose-Einstein condensates.[26] In 1998, we exploited the various new possibilities provided by optical confinement:

- Optical traps allow precise spatial (micrometer) and temporal (microseconds) manipulation of Bose-Einstein condensates. This should allow the realization of box traps, atom guides, and optical lattices. We have used the spatial resolution afforded by optical traps to create a new “dimple” trap in which BEC was created adiabatically and thus reversibly (Section 2.4.2).
- Optical traps have a new external degree of freedom: they can be operated at arbitrary external magnetic fields. We have used this feature for the observation of Feshbach resonances for strong field seeking states of sodium which cannot be confined magnetically (Sections 2.4.3 and 2.4.4).
- Optical traps offer a new internal degree of freedom: the orientation of the atom's magnetic moment. This resulted in the generation of spinor condensates, condensates which populate all three hyperfine states of the F = 1 state of sodium (Sections 2.4.6 and 2.4.7) and possess a three-component vectorial order parameter.

2.4.2 Reversible Formation of a Bose-Einstein Condensate

In an ordinary cryostat, the experimenter can raise and lower the temperature of a sample reversibly. In contrast, evaporative cooling is irreversible due to the loss of the evaporated atoms. Even if the temperature is raised again by (internal or external) heating of the sample, some number of atoms lost during the cooling stage cannot be recovered.

In recent experiments, we could cross the BEC transition reversibly by slowly changing the shape of the trapping potential using a combination of magnetic and optical forces.[28] This process conserves entropy while changing the local phase space density.

By ramping up the power of an infrared beam focused into the center of the magnetic trap, we could increase the phase-space density by a factor of 50. The reversibility of crossing the BEC phase transition was demonstrated by preparing a magnetically trapped cloud just above the critical temperature and then sinusoidally modulating the infrared power. We could reversibly cycle at least 15 times back and forth across the BEC transition (Figure 12).

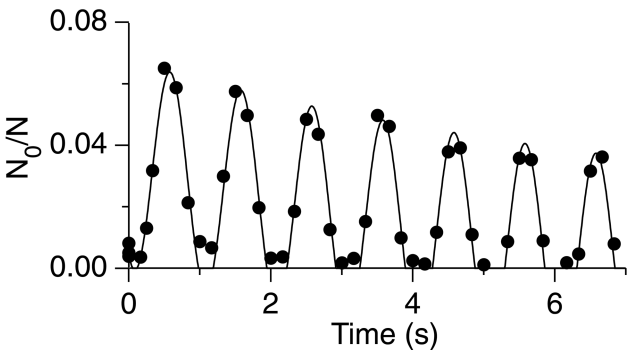

Figure 12. Adiabatic cycling through the phase transition by sinusoidally modulating the optical trapping potential. Shown is the condensate fraction versus time. The solid lines are guides to the eye.

2.4.3 Observation of Feshbach Resonances in a Bose-Einstein Condensate

All the essential properties of Bose condensed systems—the formation and shape of the condensate, the nature of its collective excitations and statistical fluctuations, the formation and dynamics of solitons and vortices—are determined by the strength of the atomic interactions. In atomic gases, the strength of the interaction, characterized by the scattering length, varies dispersively near a Feshbach resonance which occurs at a specific value of the external magnetic field.

Our recent observation of Feshbach resonances in an optically trapped condensate[29] was the first such observation for cold atoms. The strength of the interaction was inferred from the measured release energy. Figure 13 displays the predicted dispersive shape and shows evidence for a variation in the scattering length by more than a factor of ten. Our observation of the dispersive variation of the scattering length confirms the theoretical predictions about “tunability” of the scattering length with the prospect of “designing” atomic quantum gases with novel properties.

28 D.M. Stamper-Kurn, H.-J. Miesner, A.P. Chikkatur, S. Inouye, J. Stenger, and W. Ketterle, “Reversible Formation of a Bose-Einstein Condensate," *Phys. Rev. Lett*. 81: 2194 (1998).

29 S. Inouye, M.R. Andrews, J. Stenger, H.-J. Miesner, D.M. Stamper-Kurn, and W. Ketterle, "Observation of Feshbach Resonances in a Bose-Einstein Condensate," *Nature* 392: 151 (1998).

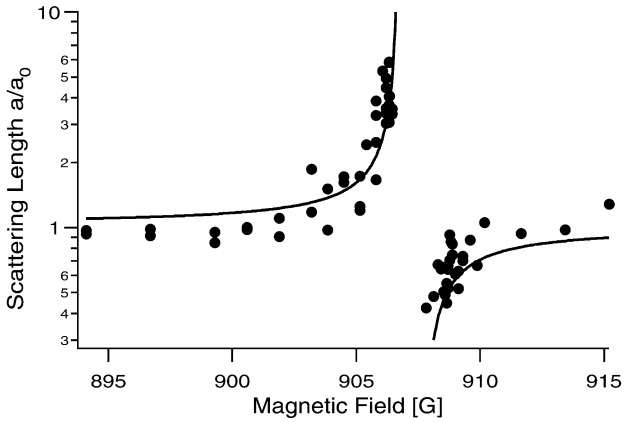

Figure 13. Observation of the Feshbach resonance at a magnetic field of 907 G using time-of-flight absorption imaging. The figure shows the normalized scattering length versus external magnetic field, together with the predicted shape.

2.4.4 Strongly Enhanced Inelastic Collisions in a Bose-Einstein Condensate near Feshbach Resonances

The properties of Bose-Einstein condensed gases can be strongly altered by tuning the external magnetic field near a Feshbach resonance. Feshbach resonances affect elastic collisions and lead to the observed modification of the scattering length. However, we found that this is accompanied by a strong increase in the rate of inelastic collisions. The observed three-body loss rate increased when the scattering length was tuned to both larger or smaller values than the off-resonant value.[30] The maximum measured increase of the loss rate was several orders of magnitude. Sweeps of the magnetic field through the resonance resulted in loss of most of the atoms in one microsecond. These observations are not explained by theoretical treatments and indicate molecular and many-body physics which is not yet accounted for. The strong losses impose severe limitations for using Feshbach resonances to tune the properties of Bose-Einstein condensates. A new Feshbach resonance in sodium at 1195 G was observed with a region of negative scattering length on the low field side. This field can therefore be directly approached without crossing any resonance.

2.4.5 Analytical Description of a Trapped Semi-ideal Bose-Gas

One focus of our research on dilute gas Bose-Einstein condensates is the study of thermodynamic quantities such as the transition temperature to Bose-Einstein condensation and the condensate fraction, which is the ratio of the number of atoms in the condensate to the total number in the gas. In particular, for the dilute gas Bose condensates, the weak interactions between particles and their low density allow for an accurate theoretical description of the effect of interactions in a many-body system starting from a microscopic understanding of two-particle collisions. In collaboration with Dr. Martin Naraschewski,[31] a member of our group, Dan M. Stamper-Kurn, explored the effect of interactions on trapped partially-condensed gas using an intuitive and accessible description of the interactions between the condensed and non-condensed atoms. In this “semi-ideal” picture, interactions between condensed atoms are treated by the simple and verified Thomas-Fermi approximation, while the uncondensed fraction is treated as an ideal gas for which the trapping potential and the chemical potential are altered by repulsion from the condensate. This led to analytical expressions for the condensate fraction and the density of the trapped gas that can be used directly in the comparison between theory and experimental data.

2.4.6 Spinor Bose-Einstein Condensates in Optical Traps

We have studied the equilibrium state of spinor condensates in an optical trap.[32] In contrast to magnetically trapped condensates, spinor condensates have the orientation of the spin as a degree of freedom which can be described by a multicomponent wavefunction (one for each magnetic sublevel). In an F = 1 spinor condensate subject to spin relaxation, two $m_F = 0$ atoms can collide and produce an $m_F = 1$ and an $m_F = -1$ atom and vice versa. The most dramatic effect was seen when we started with a condensate in a pure $m_F = 0$ state. Depending on the external magnetic field, the formation of three domains of $m_F = +1, 0, -1$ atoms was observed.

30 J. Stenger, S. Inouye, M.R. Andrews, H.-J. Miesner, D.M. Stamper-Kurn, and W. Ketterle, "Strongly Enhanced Inelastic Collisions in a Bose-Einstein Condensate Near Feshbach Resonances," *Phys. Rev. Lett.* 82: 2422 (1999).

31 Institute for Theoretical, Atomic, and Molecular Physics, Harvard-Smithsonian Center for Astrophysics, Cambridge, Massachusetts.

32 J. Stenger, S. Inouye, D.M. Stamper-Kurn, H.-J. Miesner, A.P. Chikkatur, and W. Ketterle, "Spin Domains in Ground State Spinor Bose-Einstein Condensates," *Nature* 396: 345 (1998).

Figure 14 shows a sequence of images with different dwell times in the optical trap. Starting with either the pure $m_F = 0$ component (upper series) or with a 50-50 mixture of the $m_F = \pm 1$ components (lower series), the same equilibrium distribution was reached.

Comparison of images like those in Figure 14 to a theoretical model revealed that the spin-dependent interaction $cF_1 \bullet cF_2$ between two sodium atoms in the F = 1 state is anti-ferromagnetic (i.e., c > 0). Furthermore, the experimental results showed clear evidence for the miscibility of $m_F = -1$ and $m_F = +1$ components and the immiscibility of $m_F = \pm 1$ and $m_F = 0$. This opens the possibility for detailed studies of miscible and immiscible multicomponent condensates.

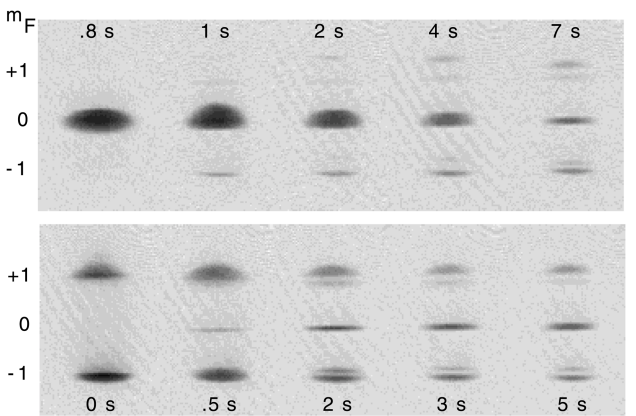

Figure 14. Absorption images of spinor condensates released from the optical trap, after 25 ms of ballistic expansion. The different m_F states were separated by an axial field gradient (Stern-Gerlach filter). The images taken after various dwell times in the trap show how the atoms evolved into the same equilibrium distribution although they were initially prepared in a pure $m_F = 0$ state (upper row) or in equally populated $m_F = \pm 1$ states (lower row). The height of the images is 2.7 mm.

2.4.7 Metastable Bose-Einstein Condensates

During the studies of the spinor ground states, we encountered two different types of metastability that we investigated in more detail.[33] In one case, a two-component condensate in the $m_F = 1,0$ hyperfine states was stable in spin composition, but spontaneously formed a metastable spatial arrangement of spin domains. In the other, a single component $m_F = 0$ condensate was metastable in spin composition with respect to the development of $m_F = +1,-1$ ground-state spin domains. In both cases, the energy barriers which caused the metastability (as low as 0.1 nK) were much smaller than the temperature of the gas (about 100 nK) which would suggest a rapid thermal relaxation. However, since the thermal energy is only available to uncondensed atoms, this thermal relaxation was slowed considerably due to the high condensate fraction and the extreme diluteness of the uncondensed cloud.

The upper part of Figure 14 shows the time evolution of a condensate initially prepared in the $m_F = 0$ state, with a metastability time of 0.8 sec. For the coldest and most diluted condensates metastability for as long as 5 sec was observed.

2.4.8 A Next-generation BEC Experiment

A major effort of our group is the design and construction of an improved source of Bose condensed atoms. The design includes an intense slow atomic beam which should result in one to two orders of magnitude improvements in the loading rates of atom traps and lead to considerably larger condensates than have been obtained so far. All major parts, including a glass trapping chamber and a tightly confining magnetic trap are assembled. The experimental setup will allow high-resolution imaging at short working distances. Laser-cooled atoms were recently transferred into the magnetic trap and will now be cooled further by evaporative cooling.

33 H.-J. Miesner, D.M. Stamper-Kurn, J. Stenger, S. Inouye, A.P. Chikkatur, and W. Ketterle, "Observation of Metastable States in Spinor Bose-Einstein Condensates," *Phys. Rev. Lett*. 82: 2228 (1999).

2.4.9 Publications

Journal Articles

Andrews, M.R., D.S. Durfee, S. Inouye, D.M. Stamper-Kurn, H.-J. Miesner, and W. Ketterle. "Studies of Bose-Einstein Condensates." *J. Low Temp. Phys*. 110: 153-66 (1998).

Durfee, D.S., C. Kuklewicz, R. Onofrio, C. Raman, J.M. Vogels, and W. Ketterle. "Experimental Study of Large Bose Condensates." *Bull. Am. Phys. Soc.* 43: 1341 (1998).

Durfee, D.S., and W. Ketterle. "Experimental Studies of Bose-Einstein Condensation." *Opt. Express* 2: 299-313 (1998).

Inouye, S., M.R. Andrews, J. Stenger, H.-J. Miesner, D.M. Stamper-Kurn, and W. Ketterle. "Observation of Feshbach Resonances in a Bose-Einstein Condensate." *Nature* 392: 151-54 (1998).

Inouye, S., M.R. Andrews, J. Stenger, H.-J. Miesner, D.M. Stamper-Kurn, and W. Ketterle. "Studies of Bose-Einstein Condensation in Various Hyperfine States." *Bull. Am. Phys. Soc.* 43: 1251 (1998).

Ketterle, W. "Optical Confinement of Bose-Einstein Condensates." *Opt. Photon. News* 9(12): 42 (1998).

Miesner, H.-J. "Recent Results on Bose-Einstein Condensation." *Bull. Am. Phys. Soc.* 43: 1253 (1998).

Miesner, H.-J., and W. Ketterle. "Bose-Einstein Condensation in Dilute Atomic Gases." *Solid State Commun.* 107: 629-37 (1998).

Miesner, H.-J., D.M. Stamper-Kurn, M.R. Andrews, D.S. Durfee, S. Inouye, and W. Ketterle. "Bosonic Stimulation in the Formation of a Bose-Einstein Condensate." *Sci.* 279: 1005-07 (1998).

Miesner, H.-J., D.M. Stamper-Kurn, J. Stenger, S. Inouye, A.P. Chikkatur, and W. Ketterle. "Observation of Metastable States in Spinor Bose-Einstein Condensates." *Phys. Rev. Lett.* 82: 2228 (1999).

Naraschewski, M., and D.M. Stamper-Kurn. "Analytical Description of a Trapped Semi-ideal Bose Gas at Finite Temperature." *Phys. Rev. A* 58: 2423-26 (1998).

Stamper-Kurn, D.M., M.R. Andrews, A.P. Chikkatur, S. Inouye, H.-J. Miesner, J. Stenger, and W. Ketterle. "Optical Confinement of a Bose-Einstein Condensate." *Phys. Rev. Lett.* 80: 2072-75 (1998).

Stamper-Kurn, D.M., M.R. Andrews, A.P. Chikkatur, S. Inouye, H.-J. Miesner, J. Stenger, and W. Ketterle. "Studies of Optically Confined Bose-Einstein Condensates." *Bull. Am. Phys. Soc.* 43: 1251 (1998).

Stamper-Kurn, D.M., H.-J. Miesner, A.P. Chikkatur, S. Inouye, J. Stenger, and W. Ketterle. "Reversible Formation of a Bose-Einstein Condensate." *Phys. Rev. Lett.* 81: 2194-97 (1998).

Stamper-Kurn, D.M., H.-J. Miesner, S. Inouye, M.R. Andrews, and W. Ketterle. "Collisionless and Hydrodynamic Excitations of a Bose-Einstein Condensate." *Phys. Rev. Lett.* 81: 500-03 (1998).

Stenger, J., S. Inouye, M.R. Andrews, H.-J. Miesner, D.M. Stamper-Kurn, and W. Ketterle. "Strongly Enhanced Inelastic Collisions in a Bose-Einstein Condensate Near Feshbach Resonances." *Phys. Rev. Lett*. 82: 2422 (1999).

Stenger, J., S. Inouye, D.M. Stamper-Kurn, H.-J. Miesner, A.P. Chikkatur, and W. Ketterle. "Spin Domains in Ground State Spinor Bose-Einstein Condensates." *Nature* 396: 345-48 (1998).

Stenger, J., D.M. Stamper-Kurn, M.R. Andrews, A.P. Chikkatur, S. Inouye, H.-J. Miesner, and W. Ketterle. "Optically Confined Bose-Einstein Condensates." *J. Low Temp. Phys.* 113: 167-88 (1998).

Meeting Papers

Durfee, D.S., C. Kuklewicz, R. Onofrio, C. Raman, J.M. Vogels, and W. Ketterle. "A New Apparatus for the Study of Large Bose-Einstein Condensates." Sixteenth International Conference on Atomic Physics (ICAP), Windsor, Canada, 1998, *Book of Abstracts*, paper B27.

Ketterle, W. "Bose-Einstein Condensation, Atomic Coherence and the Atom Laser." Sixth European Conference on Atomic and Molecular Physics (ECAMP VI), Siena, Italy, July 14-18, 1998, *Book of Abstracts*.

Ketterle, W. "The New Physics of Optically Trapped Bose-Einstein Condensates." Symposium on Quantum Fluids and Solids (QFS 98), Amherst, Massachusetts, June 9-14, 1998, *Book of Abstracts*, paper 9-S2.

Ketterle, W. "The New Physics of Optically Trapped Bose-Einstein Condensates." Annual meeting of the section for atomic physics and quantum electronics of the Dutch Physical Society, Lunteren, The Netherlands, November 5-6, 1998, *Book of Abstracts*, I4.

Ketterle, W. “Recent Advances in Bose-Einstein Condensation.” CLEO/Europe-EQEC ’98, Glasgow, Scotland, 1998, *Advance Program*, p. 30.

Miesner, H.-J., S. Inouye, M.R. Andrews, J. Stenger, D.M. Stamper-Kurn, and W. Ketterle. “Beobachtung von Feshbach-Resonanzen in einem Bose-Einstein-Kondensat.” Spring meeting of the German Physical Society 1998, *Book of Abstracts*, paper Q51.6.

Miesner, H.-J., and W. Ketterle. “Bose-Einstein Condensation in Dilute Atomic Gases and Realization of an Atom Laser.” *Proc. SPIE* 3270, Methods for Ultrsensitive Detection, ed. B.L. Fearey, ISBN 0-8194-2709-8, pp. 107-15 (1998).

Miesner, H.-J., D.M. Stamper-Kurn, M.R. Andrews, A.P. Chikkatur, D.S. Durfee, S. Inouye, J. Stenger, and W. Ketterle. “Reversible and Irreversible Formation of a Bose-Einstein Condensate.” Sixteenth International Conference on Atomic Physics (ICAP), Windsor, Canada, 1998, *Book of Abstracts*, paper B26.

Miesner, H.-J., D.M. Stamper-Kurn, M.R. Andrews, A.P. Chikkatur, S. Inouye, J. Stenger, and W. Ketterle. “Optische Falle für Bose-Einstein-Kondensate.” Spring meeting of the German Physical Society 1998, *Book of Abstracts*, paper SYA2.1.

Stamper-Kurn, D.M., M.R. Andrews, A.P. Chikkatur, S. Inouye, H.-J. Miesner, J. Stenger, and W. Ketterle. “Bose-Einstein Condensates at the Focus of an Infrared Laser.” Sixteenth International Conference on Atomic Physics (ICAP) 1998, Windsor, Canada, 1998, *Book of Abstracts*, paper B25.

Stamper-Kurn, D.M., M.R. Andrews, A.P. Chikkatur, S. Inouye, H.-J. Miesner, J. Stenger, and W. Ketterle. “Studies of Magnetically and Optically Confined Bose-Einstein Condensates.” International Quantum Electronics Conference IQEC ’98, San Francisco, California, 1998, *Advance Program*, p. 82.

Stamper-Kurn, D.M., H.-J. Miesner, A.P. Chikkatur, S. Inouye, J. Stenger, and W. Ketterle. “Bose-Einstein Condensation by Adiabatic Compression.” OSA Annual Meeting, Baltimore, Maryland, 1998, *Book of Abstracts*, paper WLL4.

Chapter in a Book

Ketterle, W. “Atom Laser.” In *McGraw-Hill 1999 Yearbook of Science and Technology.* New York: McGraw-Hill, 1998.

Doctoral Dissertation

Andrews, M.R. *Bose Condensates and the Atom Laser.* Ph.D. diss. Department of Physics, MIT, 1998.